Hindawi
International Journal of Antennas and Propagation
Volume 2023, Article ID 7157721, 15 pages
https://doi.org/10.1155/2023/7157721

Research Article

Measurement-Based Analysis on Vehicle-to-Vehicle Connectivity in Tunnel Environment

Suying Jiang,[1,2] **Wei Wang**,[1] **Ibrahim Rashdan**,[3] **Paul Unterhuber**,[3] **and Peng Peng**[4]

[1]*School of Information Engineering, Chang'an University, Xi'an, China*
[2]*School of Electronic and Electrical Engineering, Baoji University of Arts and Sciences, Baoji, China*
[3]*Institute of Communications and Navigation, German Aerospace Center (DLR), Oberpfaffenhofen, Germany*
[4]*School of Electrical and Control Engineering, Shaanxi University of Science and Technology, Xi'an, China*

Correspondence should be addressed to Wei Wang; wei.wang@chd.edu.cn

Received 20 December 2022; Revised 10 February 2023; Accepted 20 February 2023; Published 7 March 2023

Academic Editor: Sandeep Kumar Palaniswamy

Vehicular ad hoc network (VANET) brings an excellent solution to ensure road safety and transportation efficiency in critical environment like tunnel. Particularly, radio link connectivity of vehicle-to-vehicle (V2V) significantly influences the performance of VANETs. The communication range of the radio systems is a random variable in reality due to the channel fading effect. Therefore, the connectivity model between vehicles in realistic environment is a key for accurate evaluation of system performances. In this paper, we study the V2V connectivity performance in the presence of channel randomness for tunnel environment. Firstly, based on channel measurement campaign, empirical path loss (PL) and small-scale fading channel models are established. Secondly, we study the influence of large-scale fading parameters on V2V connectivity. Thirdly, based on real small-scale fading characteristics, we derive the V2V connectivity probability between any two vehicles under Nakagami fading channel for one-dimensional VANET, and give the closed-form of V2V connectivity probability. Finally, we study the influences of various parameters (i.e., Nakagami fading factor, vehicle density, and neighbor order) on V2V connectivity performance. Results show that with the Nakagami fading shape factor increases, the connectivity probability increases. The shadowing fading can improve connectivity in the VANET; the path loss exponent, transmission distance, and signal-to-noise ratio (SNR) threshold have a negative impact on connectivity probability. The transmit power, vehicle density, and path loss threshold value have a positive impact on connectivity.

1. Introduction

Vehicular ad hoc network (VANET) is a subset of the mobile ad hoc network (MANET); it includes self-organizing vehicle and roadside infrastructure. In the VANET, vehicles and infrastructures are equipped with wireless communication equipment for real time information exchange, which is a fundamental of the efficient and safe intelligent transportation system [1–3]. Particularly, the radio link connectivities of vehicle-to-infrastructure (V2I) and vehicle-to-vehicle (V2V) is a key metric to assess the VANET communication performances in terms of both communication range and vehicle networking that strongly affect advanced techniques like cooperative communication and positioning. Therefore, it is a meaningful work to study the connectivity in the VANET.

Due to factors like propagation loss, the dynamic characteristic of VANET topology, high speed of vehicle movement, and the occlusion of other vehicles, the received signal strength of a specific link changes rapidly, even drops down below the level of system sensitivity. As a result, established communication links may be interrupted or even lost. Over the past years, the connectivity of VANETs has been extensively studied, where the research focuses on the following aspects: (1) the influence of traffic and weather factors on connectivity (e.g., the traffic flow, vehicle density,

the distribution of vehicle and its speed, weather conditions, and traffic lights); (2) the effect of wireless propagation environments on connectivity (e.g., path loss (PL) model, Nakagami fading, Weibull fading, Rice fading, Rayleigh fading, and communication range); (3) different modelling approaches of connectivity; (4) performance enhancing method of connectivity, such as the deployment of roadside unit (RSU), and multihop communications.

Several research studies mainly concentrate on the impacts of various factors on VANET connectivity. In [4, 5], the influences of communication range, vehicle speed, the safe distance, size of vehicle, traffic lights, and overtaking of vehicles on connectivity were analyzed. The dependency between the connectivity of the VANET and mobility was studied in [6–13]. In [11], authors analyzed the effects of vehicle mobility on the VANET connectivity probability based on a measurement data set. Simulation results showed that the connectivity probability decreases with a power-law decline if vehicle speed is greater than certain threshold, whereas the connectivity is not affected if the vehicle speed is below the threshold. In [14–16], the authors analyzed the impacts of transmission ranges of both base station (BS) and vehicle, vehicle density, and the distance between adjacent BSs on connectivity performance given different communication channel models, specifically, unit disk (UD) model and log-normal shadowing model. When studying the factors that affect the connectivity of the VANET, the impact of user behavior on connectivity cannot be ignored. The effect of user behavior on V2V and V2I connectivity was analyzed in [17, 18].

Besides, wireless propagation environments have shown to have significant impact on the connectivity. In [17, 19–26], theoretical fading models (e.g., Rayleigh, Rice, Weibull, and Nakagami) were considered, based on which the authors presented analytical models. Moreover, the impacts of different channel parameters (e.g., shadow fading, PL exponent, and small scale fading parameters) on the link connectivity probability of the VANET were studied in these papers. In [27], the dual-slope PL model and its impact on the V2V connectivity are evaluated. Results showed that the connectivity probability is higher in the line-of-sight (LoS) environment than in the obstructed line-of-sight (OLoS) environment in shorter transmission distance; in longer transmission distance, the V2V connectivity probability is higher in the OLoS environment than that in the LoS environment. A larger path loss exponent may result in a smaller connectivity probability [28]. In [24, 25, 29], the effect of lognormal shadowing on connectivity probability was analyzed. It is shown that lognormal shadowing can improve the VANET connectivity.

The previous work on the connectivity performance analysis of the VANET mainly based on queuing theory [30–34] or geometric-assisted analytical models [35]. Recently, a lot of analytical models were developed for analyzing the connectivity probability in the VANET. In [36], authors presented a connectivity model to estimate the downlink and uplink connectivity performances for the infrastructure-based VANET. Based on the path loss model, small-scale fading, and traffic flow model, a continuous connectivity model was developed [1, 37]. In [38, 39], under the assumption that the entrance and exit of the highway are uniformly distributed and the vehicle arrival process can be viewed as obeying the Poisson distribution. In [40], the vehicular network was simplified and modeled as geometric elements of lines and points. In addition, authors assumed that the arrival of vehicles obeys Poisson distribution, and analyzed the capacity and connectivity performance between two adjacent RSUs in the highway scenario. In [41], authors took into account the vehicles mobility and the large-scale channel fading, the moving vehicles were divided into clusters, and a clustering assumption based analytical model was proposed. The proposed model includes two parts, namely, catch-up process and forwarding process. In [42], the cell transmission model was adopted to capture macroscopic traffic flow dynamics, and study the connectivity performance in the freeway environment.

Both vehicle movement and channel fading have an impact on vehicle connectivity [19–22, 27, 28, 41–46]. Considering both the mobility of vehicles on the road and the characteristics of channel fading can make us have a deep understanding of the VANET connectivity performance. Some authors considered both vehicle mobility and channel fading to study the influences of various parameters on connectivity probability [21, 23]. Then, we aim to discuss the research on the influence of small scale fading on vehicle connectivity in this paper. In [21], authors considered channel fading characteristics, and derived the connectivity probability of two consecutive vehicles in one dimensional (1D) VANET under channel randomness, specifically, Rayleigh, Rice, and Weibull fading channels. In [22], authors presented the V2V connectivity probability of two consecutive cars in the 1D VANET under the Nakagami fading channel. These authors only considered the connectivity of two consecutive vehicles in the 1D VANET, they did not consider connectivity between any two vehicles. However, in the real VANET, sometimes two vehicles will be blocked by other vehicles or barriers. In this case, the density of vehicles and the degree of channel fading will be different, so the connectivity between two vehicles will also be different. The study on connectivity probability between two consecutive vehicles is not suitable for the analysis of vehicle connectivity between any two vehicles. Hence, it is meaningful to study the connectivity between any two vehicles. However, there is little research on V2V connectivity probability of any two vehicles under the small-scale fading channel. Although authors proposed the probability of any two cars are connected under the Rayleigh channel in [23], Rice, Weibull, and Nakagami fading channels were not considered. It is very important to study the connectivity performance between any two vehicles under small-scale fading in OLoS and non-line-of-sight (NLoS) cases.

Table 1 summaries various connectivity models and corresponding parameters considered in the literature. The research studies on vehicle connectivity mainly focus on urban [55, 65], highway [47, 51, 66], and intersection scenarios [53, 58, 59]. There are very few studies on vehicle connectivity for the tunnel scenario that is a critical use case in the traffic system. In [47], the minimal safe distance was considered, and the connectivity was analyzed in a highway tunnel, where, however, only the vehicle transmission range

and vehicle density were considered without incorporating the channel fading effect. Furthermore, in realistic OLoS and NLoS scenarios, the fading of signal amplitude usually does not follow the ideal Rayleigh distribution due to the complex propagation environment. In outdoor environment, it has been reported that fading of signal amplitudes usually follow distributions with higher degree of freedom like Weibull and Nakagami distributions. However, there exist very limited research studies of the small-scale fading model for the tunnel environment.

In this work, we focus on filling the gap in analyzing the connectivity performance in a more generalized scenario for the tunnel environment, i.e., between any two vehicles (two vehicles are blocked by other vehicles) where the traditional connectivity model between two consecutive vehicles is not suitable anymore. As a key contribution, we take into account a more realistic small-scale fading model rather than the Rayleigh distribution to derive the connectivity probability. We extend the study in [22] from two adjacent vehicles to any two vehicles. Based on the channel measurement data in a typical tunnel scenario in Munich, Germany, we analyze the small-scale fading characteristics. Measurement results show that the Nakagami-m distribution is the best fitted fading model for the tunnel environment. Thereafter, the connectivity probability between any two vehicles under Nakagami-m and log-normal shadow fading channels for a 1D VANET is derived. Furthermore, we analyze the influences of Nakagami-m fading, large-scale fading, and traffic parameters on V2V connectivity.

The key contributions of this paper are summarized as follows:

(i) A well calibrated channel measurement campaign was carried out in a typical tunnel environment in Munich, Germany. The signal amplitude is found to experience the Nakagami-m fading rather than Rayleigh fading.

(ii) Based on the small-scale fading characteristics obtained from the measurement data in the tunnel, we propose a closed-form connectivity probability between any two vehicles under the Nakagami-m channel and log-normal shadowing channel for a one-dimensional VANET. Furthermore, we also analyze the effects of the Nakagami fading factor, the neighbor order, and the threshold value of received SNR on connectivity performance.

(iii) We study the influences of large-scale fading parameters on VANET connectivity. We demonstrate that the shadowing fading has a positive impact on V2V connectivity.

The rest of this paper is organized as follows: in Section 2, a channel measurement campaign in the tunnel is described. Thereafter, the PL and small-scale fading characteristics are studied in Section 3. The V2V connectivity probability considering the PL model is presented, and the influences of large-scale fading parameters on V2V connectivity are analyzed in Section 4. We propose the V2V connectivity probability model between any two vehicles under Nakagami fading for a one-dimensional VANET in Section 5. Moreover, we discuss the influences of various parameters on V2V connectivity probability in this section. Finally, some concluding remarks are described in Section 6.

2. Channel Measurement Campaign

To study the channel propagation characteristics in tunnels, we conducted the channel measurement campaign in a tunnel, as shown in Figure 1. Figure 1 illustrates the measurement environment; the tunnel is located close to the city of Munich, Germany. During the measurement process, a Medav RUSK-DLR broadband channel sounder was used to measure the channel characteristics data, and obtain the channel frequency response (CFR). The orthogonal frequency division multiplexing (OFDM) signal was emitted by the transmitter at a center frequency of 5.2 GHz. The bandwidth of the signal is 120 MHz. The receiver received the CFR $H(t_k, f_z)$, where $t_k = k \cdot t_j$, t_j is the measurement time grid, k denotes the time index of the measured data, $k = 1, 2, 3, \cdots$, and f_z is the frequency associated with the bin z, $z = 0, 1, \ldots, N-1$, where N stands for the subcarrier's number. We can acquire the complex channel impulse response (CIR) $h(t_k, \tau_z)$ by taking the inverse Fourier transform of CFR $H(t_k, f_z)$, where $\tau_z = z \cdot \tau_\Delta = z/B$, B is the bandwidth, τ_Δ denotes the delay resolution, and $\tau_\Delta = 1/B$. Table 2 summarizes the channel measurement parameters.

During the measurement, the transmitter was in one car and the receiver was in the other car; the transmitting and receiving antennas were mounted on the roof of two vehicles. The rubidium atomic clock is widely used to achieve time synchronization between the receiver and the transmitter. Without loss of generality, we also made use of two rubidium atomic clocks on the transmitter and receiver side. In order to obtain the ground truth of distance between the receiver and transmitter, accurate position information are essential. However, due to the nature of the tunnel, signal blockage by concrete walls handicaps the successful receiving of global navigation satellite system (GNSS) signals. Therefore, ground-based augmentation approach is considered. Both transmitter and receiver were equipped with GNSS receivers, together with the inertial measurement unit (IMU) and LIDAR. Therefore, it is possible to combine all different sensor measurements to acquire the positions of the vehicle.

Two cars were travelling in the same direction in the tunnel. In addition, the speed and the distance between two vehicles vary with the actual density of the traffic flow during the channel measurement. For the LoS scenario, there exists a clear visual LoS path between the receive antenna (RX) and transmit antenna (TX). For the OLoS scenario, the LoS path between receive antenna and transmit antenna is partially blocked by other cars with small sizes. As for the NLoS scenario, there exist vehicles with large sizes (e.g., bus, van, and truck) located in between the RX and TX such that the visual LoS path is completely blocked. The vehicle carrying the transmitter is called the transmitting vehicle and the

Table 1: Connectivity models.

Reference	System model	Parameters	Scenarios	Measurement
[4]	Car following model	Communication range, vehicle speed, the length of vehicle, the safe distance, and traffic lights	Urban road with intersections	No
[5, 18, 47]	The vehicle speed follows Gaussian distribution and the arrival time of vehicles obeys an exponential distribution	Communication range, vehicle speed, density and arrival rate, the ratio of active cars, the vehicle safety distance, user behavior, the ratio of cars transmit signals, and the distance between two adjacent RSUs	A two-way lane and an one-wayone-lane highway	No
[6]	A unit disk graph radio connectivity model	Vehicle movements, transmission range, and the number of neighbors	Highway	Yes
[7, 38–40, 48]	The arrival of vehicles obeys the Poisson distribution	Vehicle movements, transmission range, velocity, the probability of a car passing through the entrance or exit, and vehicle arrival rate	Highway	No
[8]	The arrival of vehicles obeys a Poisson distribution and the adjacent vehicle arrival time and the adjacent vehicle distance follow the exponential distribution; generalized speed factor system model	The number of road lanes, vehicle density and speed, transmission range, the vehicular mobility, and the vehicle arrival rate	Highway	No
[11]	A simple unit disk model	The vehicular speed, communication range, and the component speed and size	Urban	Yes
[14, 15, 49]	A Poisson distribution, a UD model; log-normal shadowing model	The coverage range of BSs and vehicles, vehicle density, inter-BS distance, multihop communication, average length of vehicles, minimum safety headway, the distribution of vehicles, and one-hop transmission range	A road	No
[16]	A multipriority Markov model	The coverage of RSUs and vehicles, traffic density, the platoon ratio of VANET, and the distance of adjacent RSUs	One-way road and two-way road	No
[17]	The arrival of vehicles obeys a homogeneous Poisson process; Nakagami distribution	User behavior, active vehicle ratio, traffic flow, and the channel fading factors	Highway	No
[50]	The arrival of vehicles follows homogenous Poisson process; Nakagami-m distribution	Nakagami fading parameter, transmission power, PL exponent, and signal-to-noise ratio (SNR) threshold value	A road	No
[51]	In free-flowing traffic and congestion conditions, the headway distance follows the exponential distribution and the Gaussian unitary ensemble distribution, respectively; Nakagami-m model	Headway distance and vehicle density	Highway	Yes
[52, 53]	Path loss model	Adverse weather conditions, traffic density, communication range, and path loss threshold value	A two-lane road; intersection	Yes
[19–25]	A queuing theoretic model, path loss model, Nakagami, Rayleigh, Weibull, and rice fading model	PL exponent, shadow fading, fading factors, vehicle density, vehicle speed, vehicle arrival rate, transmission range, and received SNR threshold	Highway	No
[1, 37]	Traffic flow model, path loss model, and small-scale fading model	Different traffic flows and effective communication coverage	Highway	Yes
[27, 28]	The dual-slope path loss and traffic flow model	Path loss exponent, traffic flow, and intervehicle distance	Urban; highway	No
[30, 31]	An equivalent traffic model based on queuing theory	Transmission range, traffic parameters, and transmission range	Unidirectional lane road; highway	No

Table 1: Continued.

Reference	System model	Parameters	Scenarios	Measurement
[10, 32]	Two mobility models	The mobility pattern, transmission range, bus routes, traffic lights, and background traffic	Streets	No
[36, 54]	The Poisson traffic model, the UD model, and log-normal shadowing model	Distance between adjacent BSs, radio coverage range of vehicle, traffic density, the number of roadside infrastructure, data sinks, the maximum number of hops in a propagation path, and intervehicle distance	The road between two adjacent BSs	No
[41]	The cluster-based analytical model, the UD model, and log-normal shadowing model	Propagation distance, vehicle density, the distribution of vehicle, one-hop transmission range, and the minimum safety distance of two adjacent cars	Highway	No
[55]	Dynamic clustering model, the adjacent vehicle distances follow the exponential distribution, and the distribution of vehicles obeys the homogenous Poisson distribution	Vehicle driving, vehicle speed, and the traffic environment features	Urban	No
[56]	The arrival time of vehicles obeys exponential distribution and the vehicle speed follows the Gaussian distribution	Vehicle density, vehicles communication range, and the minimum safety distance	A two-lane road	No
[57]	The exponential distribution model and generalized extreme value (GEV) distribution	Intervehicle spacing distribution and vehicle density	Highway	No
[42]	The cell transmission model and Rayleigh distribution	The vehicle flow, the message size, the communication radius, the path loss exponent, and the data rate	Freeway	No
[58]	A new cellular automata-based mobility model	Traffic density	Urban intersection	No
[59]	The triangular model	The transmission range, vehicle density, and street width	Intersection	No
[60]	BA-realtime, BA-realtime + TL, and BA-fullroad	Vehicle mobility model, vehicle density, vehicle speed, transmission range, and the position and number of RSUs	A road	No
[61]	Microscopic mobility and lane changing decision model	Network metric data delivery rate, vehicle density, velocity and arrival rate, deceleration or acceleration, and the safety gap	Highway	No
[62]	Microscopic models	Communication range, vehicular density, the number of highway lanes, and the speed and specific daytime	Highway	No
[63]	Graph metrics	Vehicle rerouting capacity	—	No
[64]	The bond percolation model and Bollobas model	Vehicle density and transmission range	—	No

Figure 1: Measurement environment.

Table 2: Channel measurement parameters.

Parameter	Value
Center frequency	5.2 GHz
Transmit power	Max. 37 dBm
Bandwidth B	120 MHz
Measurement type	SISO
Signal period	12.8 μs
Number of carrier	1537
Measurement time grid	1.024 ms
Transmit antenna height	2 m
Receive antenna height	1.88 m
Transmit and receive antenna	Omnidirectional
Position measurement	GNSS, IMU, and LIDAR
Measurement scenarios	Tunnel

vehicle carrying the receiver is called the receiving vehicle. The camera is located in the transmitting vehicle. Based on the video information, we can know whether there are other vehicles obscured between the TX and RX during the channel measurement and the size of the obscured vehicles. We determined the LoS, OLoS, and NLoS scenarios by manual calibration. During the measurement, the receiving vehicle is in front and the transmitting vehicle is behind. When analyzing the video information, if there are other vehicles obscured between the TX and the RX, draw a circle with a certain radius taking the receiving vehicle in the video as the center, and if the receiving vehicle in front can be seen, we consider it as an OLoS scenario. When the receiving vehicle in front cannot be seen, we consider it as the NLoS scenario. In other words, when transmitting and receiving vehicles are obscured by small cars between them, the receiving vehicle is not completely obscured; this scenario can be seen as the OLoS scenario. When the transmitting and receiving vehicles are obscured by large trucks, the receiving vehicle is completely obscured, this scenario can be seen as the NLoS scenario. When analyzing the video information, if there are no other vehicles obscured between the transmitter and the receiver, there is a LoS path; this scenario can be seen as the LoS scenario. Combining the real time of channel measurement campaign, we can estimate the real time of LoS, OLoS, and NLoS scenarios. Through channel measurement, we can obtain CFR data and the time information of the CFR signal. The obtained CFR data can be converted to CIR data. Each CIR has a corresponding real time information. Based on the obtained time information of LoS, OLoS, and NLoS, we can divide the collected CIR data into LoS, OLoS, and NLoS scenarios.

Figure 2 shows the LoS scenario in the tunnel. Figure 3 depicts the OLoS scenario in the tunnel, where the LoS path is obstructed by small cars. Figure 4 illustrates a NLoS scenario in the tunnel. The transmitter and the receiver were obstructed by a blue van as shown in Figure 4, where the receiver was travelling in front of the blue van.

3. Measurement-Based Results

In this section, we aim to study the large-scale and small-scale fading characteristics based on the measured data in the tunnel.

3.1. Path Loss and Shadow Fading. The log-distance PL model in [67] is a widely used propagation model to describe the power loss during transmission; it is defined as follows:

$$P_L(d) = \varepsilon + 10n \log_{10}(d) + X_\sigma, \quad (1)$$

where d stands for the distance between RX and TX, $P_L(d)$ stands for the PL at distance d, ε represents a constant reference value, n represents the PL exponent and is the shadowing fading, which is usually a random variable that follows a zero-mean Gaussian distribution (in dB scale), and its standard deviation is σ.

In combination with the video information obtained during the channel measurements, the measurement data can be split into three independent data sets, namely, LoS condition, OLoS condition, and NLoS condition. We estimate the parameters (i.e., n, ε, and σ in equation (1) of the path loss model using the least square method. The measurement PL and theoretical PL model for different scenarios are depicted in Figures 5–7.

Generally, shadow fading in the dB scale usually follows a zero-mean Gaussian distribution [68, 69]. The shadow fading values are extracted from measurement data, and fitted with a Gaussian distribution. The extracted PL model parameters for different environments are listed in Table 3. It illustrates the PL exponent n in LoS cases, and it is smaller than the n in OLoS and NLoS cases. Because of the waveguide effect in the tunnel, the obtained PL exponent n in the tunnel is less than the value in free space. This conclusion is consistent with theory in [70].

3.2. Small-Scale Amplitude Fading Modelling. To mitigate the influence of large-scale fading, a sliding window of 50 wavelengths in length was utilized to average and normalize the power. We estimate the distribution of the received signal amplitudes. We statistically modeled the received amplitudes distribution using six different distributions, which are widely utilized in V2V scenario, such as Rayleigh distribution, Rice distribution, normal distribution, log-normal distribution, Nakagami-m distribution, and Weibull distribution. The Kolmogorov–Smirnov (KS) test with a confidence level 95% is applied to identify the best fit

Figure 2: LoS scenario.

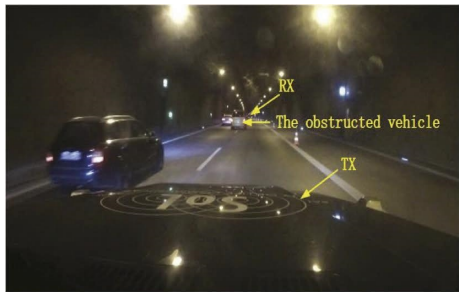

Figure 3: OLoS scenario.

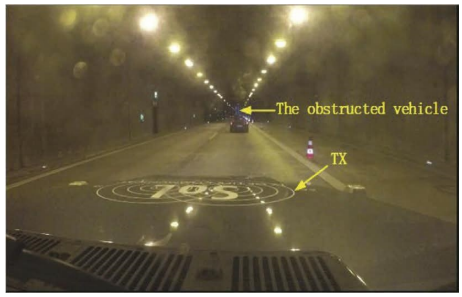

Figure 4: NLoS scenario.

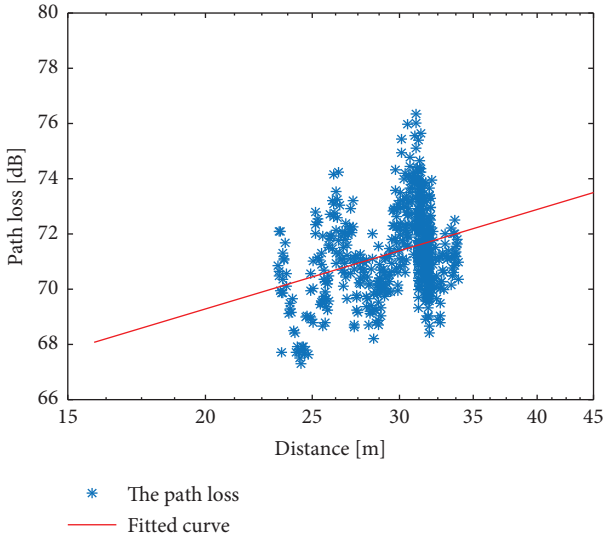

Figure 5: The path loss model for LoS scenario in the tunnel.

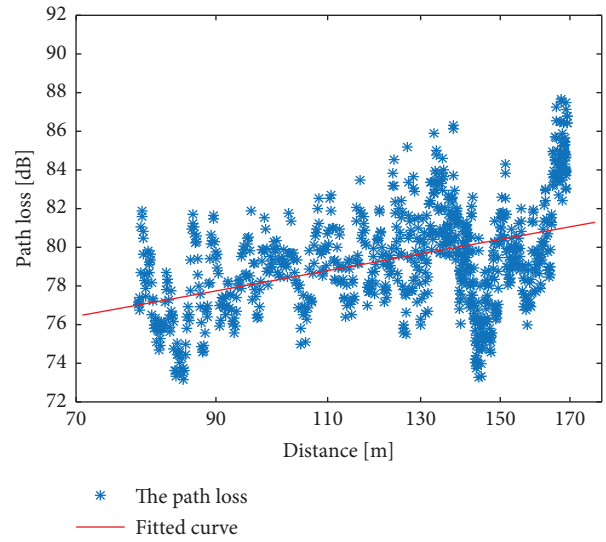

Figure 6: The path loss model for OLoS scenario in the tunnel.

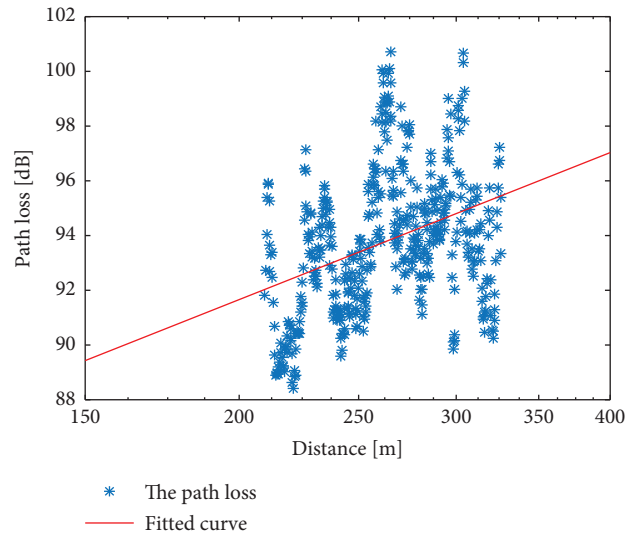

Figure 7: The path loss model for NLoS scenario in the tunnel.

Table 3: Parameters for the PL model.

Scenarios	n	ε	σ
LoS	1.196	53.719	1.458
OLoS	1.265	52.96	2.23
NLoS	1.785	50.595	2.385

distribution function [71]. The goodness of fit (GoF) value of the KS test is usually used to evaluate the best fit of a distribution. The GoF value can be calculated by $\xi = \sup_h |F_H(h) - F(h)|$, where $\sup_h$ stands for the supremum operator and $F(h)$ and $F_H(h)$ denote the theoretical and empirical cumulative distribution functions (CDFs) of the measurement data h, respectively. The lower GoF value indicates a better fit for the model.

Table 4 illustrates the obtained GoF values of various distributions. It can be seen that the Nakagami-m distribution has the smallest GoF value in the LoS, OLoS, and NLoS cases. Results showed that the Nakagami-m distribution is suitable for describing channels' randomness in the tunnel environment. This finding is consistent with the results in [72, 73].

4. Large-Scale Fading Model and Connectivity

In the VANET, the vehicles transmit information through multihop communication, therefore the connectivity of the VANET is very important in determining VANET communication capacity [11]. Moreover, the connectivity of the vehicular network is correlated with positioning accuracy of the vehicle and Cramer–Rao lower bound of localization in VANETs [74], improvement of connectivity probability is helpful to improve vehicles' positioning accuracy. Therefore, VANET connectivity is a meaningful topic, and it is widely studied. In this section, we firstly discuss modelling approach of V2V connectivity based on log-distance path loss model. Secondly, based on simulations, we present the influence of large-scale fading on V2V connectivity.

4.1. Single-Link Connectivity Probability. In VANETs, each vehicle can be seen as a transmission node. The distance between two vehicles denotes d. We define that these two vehicles are connected when the PL is less than the PL threshold value P_t, saying the received power is still above the sensitivity level of a system so that the signal can be detected and retrieved. Given the log-distance PL model in (1), the V2V connectivity probability $P_c(d)$ of any two vehicles at a distance d is defined as follows:

$$\begin{aligned} P_c(d) &= P\{P_L(d) < P_t\} \\ &= P\left\{\varepsilon + 10n\log_{10}(d) + X_\sigma < P_t\right\} \\ &= 0.5\mathrm{erfc}\left(\frac{\varepsilon - P_t + 10n\log_{10}(d)}{\sqrt{2}\,\sigma}\right), \end{aligned} \tag{2}$$

where n denotes the path loss exponent, ε denotes a constant reference value, d stands for the distance between the receiver and transmitter, σ denotes the standard derivation of shadowing fading, and P_t is the path loss threshold value. When the P_L is larger than path loss threshold P_t, the received signal is too weak to be detected. As a consequence, the radio connection is lost between these two vehicles. $\mathrm{erfc}(\cdot)$ is a complementary error function, which is written as follows:

$$\mathrm{erfc}(t) = \frac{2}{\sqrt{\pi}}\int_t^\infty e^{-x^2}\mathrm{d}x. \tag{3}$$

Due to the monotonicity of the function $\mathrm{erfc}(\cdot)$, it indicates that the PL exponent has a negative effect on connectivity performance. The PL threshold and shadow fading have a positive impact on V2V connectivity performance.

4.2. Influence of Large-Scale Fading on Connectivity. Based on the measurement results, we discuss the influence of large-scale fading parameters on vehicle connectivity performance. In this subsection, we set simulation parameters based on the estimated parameters of the PL model in the NLoS scenario. We set $\varepsilon = 50.595$, the shadow fading standard deviation $\sigma = 2.385$, path loss exponent $n = 1.785$, PL threshold value P_t ranges from 60 dB to 100 dB, and transmission distance ranges from 1 m to 1000 m. Figure 8 presents the impacts of the path loss threshold value and transmission distance on connectivity probability. It indicates that as the distance between RX and TX gradually increases, the V2V connectivity probability gradually decreases. If the PL threshold value increases, the V2V connectivity probability increases.

Figure 9 depicts the influence of the PL exponent n on V2V connectivity, in which the simulation parameters are given as follows: $\varepsilon = 50.595$, the standard deviation of shadow fading 2.385, intervehicle distance $d = 200$ m, and the PL exponent n ranges from 1 to 2.5. The setting of the path loss threshold value is related to many factors, such as transmit power, the system bandwidth, and system requirements. In this paper, we set the path loss threshold value $P_t = 90$ dB. It can been that connectivity probability decreases when n increases.

Figure 10 illustrates the influence of shadowing parameter σ on V2V connectivity, in which the path loss exponent $n = 1.785$ and the shadowing parameter σ ranges from 0.1 dB to 10 dB. It shows that the larger the shadow fading standard deviation σ is, the higher the V2V connectivity probability becomes. Therefore, it is concluded that shadow fading standard deviation σ can improve connectivity performance. This conclusion is in agreement with the earlier finding, in which the greater shadow fading standard deviation σ leads to higher connectivity performance of VANETs [20, 24].

5. Small-Scale Fading Model and Connectivity

Based on the measured data, results show that the channel in tunnel experiences the Nakagami-m distribution. However, the analysis of V2V connectivity between any two vehicles under the Nakagami channel in tunnels has not yet been studied. In this section, firstly, we derive a closed-form connectivity probability between any two vehicles under the Nakagami-m channel for a one-dimensional VANET, which has not been given in the literature. Secondly, based on the proposed connectivity model, we discuss the influences of Nakagami-m fading parameters on V2V connectivity.

5.1. Traffic Flow Model. We take into account the 1D VANET, the vehicles are in a free-flow state in the network, so the vehicle movements are independent of each other. For the free-flow traffic model, the number of vehicles passing through the observation point obeys the Poisson distribution. The arrival time of adjacent vehicles obeys the exponential distribution. The distance between two consecutive

Table 4: The GoF for different distributions.

Scenario	Normal	Log-normal	Rayleigh	Rice	Weibull	Nakagami-m
LoS	0.0228	0.0351	0.3808	0.0247	0.0625	0.0184
OLoS	0.0676	0.0729	0.0814	0.0610	0.0548	0.0489
NLoS	0.1084	0.1044	0.0833	0.0902	0.0889	0.0829

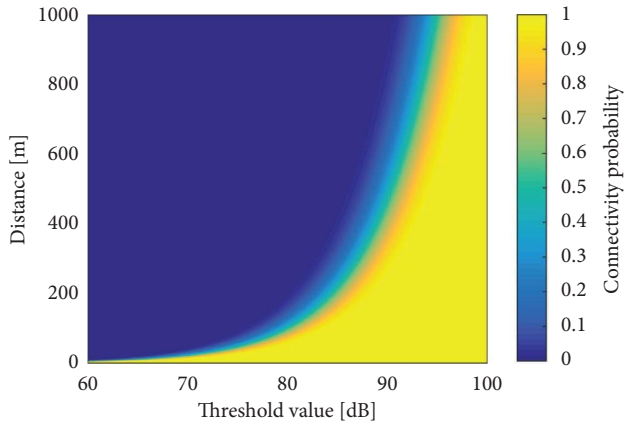

Figure 8: The impacts of path loss threshold value and transmission distance on connectivity probability in NLoS scenarios.

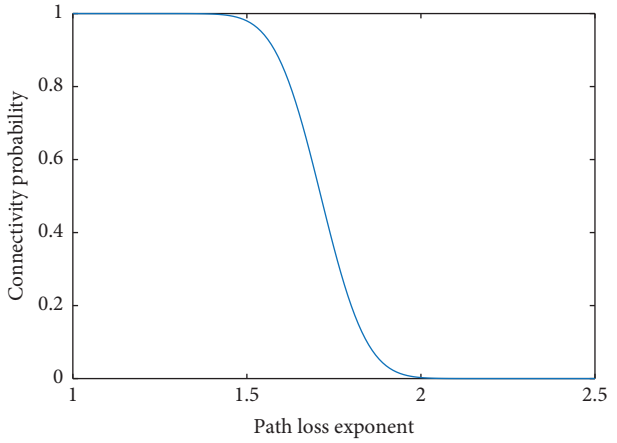

Figure 9: The effect of PL exponent n on V2V connectivity.

vehicles obeys an exponential distribution, we define it as the adjacent vehicle distance. In the VANET, because two vehicles may be obscured by other vehicles, the distance of any two vehicles has a different meaning than the distance of two adjacent vehicles, and we need to distinguish between these two cases. So, the distance between any vehicles can be defined as intervehicle distance. In this paper, X_j is a random variable representing the distance between the j-th car and the $(j+1)$-th car. The probability density function (PDF) of X_j is as follows:

$$f_{X_j}(x) = \rho e^{-\rho x}, \ (x \geq 0), \tag{4}$$

where ρ denotes average vehicle density.

Under the free-flow state, it is assumed that the vehicle speed is a discrete-time stochastic process, which obeys the

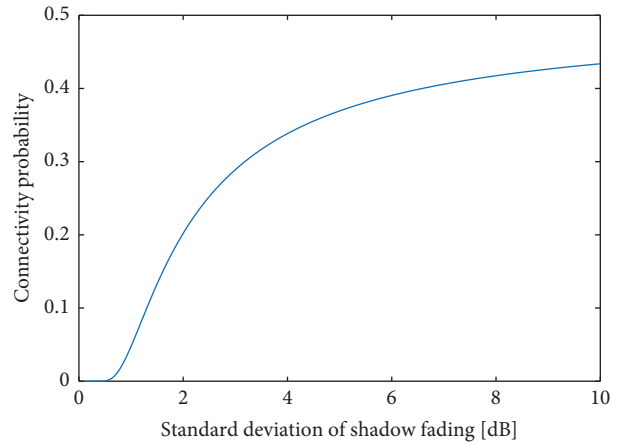

Figure 10: The impact of σ on connectivity probability.

Gaussian distribution. We focus on the tunnel environment where speed limitation is usually applied due to safety reasons. Therefore, in this paper, we assumed that the vehicle speed obeys a truncated Gaussian PDF, which can be calculated by [12]:

$$g(v) = \frac{f(v)}{\int_{v_{\min}}^{v_{\max}} f(v)\mathrm{d}v}, \ (v_{\min} \leq v \leq v_{\max}), \tag{5}$$

where $v_{\min}$ denotes the lower bound of velocity and $v_{\max}$ stands for the upper bound of velocity. In equation (5), $f(v)$ can be defined as follows:

$$f(v) = \frac{1}{\sigma_v \sqrt{2\pi}} \exp\left(\frac{-(v-\mu_v)^2}{2\sigma_v^2}\right), \tag{6}$$

where σ_v stands for the standard deviation of velocity, μ_v represents the average velocity, $v_{\max} = \mu_v + 3\sigma_v$, and $v_{\min} = \mu_v - 3\sigma_v$. Then, equation (5) can be written as follows:

$$g(v) = \frac{2f(v)}{\mathrm{erf}\left(v_{\max} - \mu_v/\sigma_v\sqrt{2}\right) - \mathrm{erf}\left(v_{\min} - \mu_v/\sigma_v\sqrt{2}\right)}, \tag{7}$$

where $v_{\min} \leq v \leq v_{\max}$, $\mathrm{erf}(\cdot)$ represents the error function, and v denotes the vehicle speed.

We define the distance between one vehicle and its q-th neighbor as the intervehicle distance Z_q. Generally, by calculating the sum of q adjacent vehicle distances X_i, we could obtain the intervehicle distance Z_q. As a result, the intervehicle distance can be calculated as $Z_q \triangleq \sum_{i=1}^{q} X_i$. The PDF of Z_q is given by [23]:

$$f_{Z_q}(x;q) = \frac{\rho^q}{(q-1)!} x^{q-1} e^{-\rho x}, \tag{8}$$

where ρ stands for the average vehicle density, q represents the neighbor order, and $(\cdot)!$ stands for the factorial operator.

5.2. Connectivity in Nakagami-m Fading Channels. According to the measurement results in Section 3, it is found that the Nakagami-m distribution can describe the fast fading well in the tunnel. In addition, it has been proven that compared to other considered fading models (i.e., Rayleigh, Weibull, and Rice), the Nakagami-m distribution is the most suitable model to represent the V2V channel randomness in both NLoS and LoS VANET environments [71]. Therefore, the analysis of the connectivity performance under Nakagami-m fading is meaningful for the design of Internet of vehicles system in the tunnel. In the following, the mathematical representation of V2V connectivity probability under the Nakagami-m channel is presented.

The probability of two nodes correctly send and receive signals can be represented as a function of the received SNR. When the distance between the receiver and transmitter is d, the SNR at the receiver is calculated by [23]

$$\gamma(d) = \frac{W^2 \beta P_T}{d^n P_{\text{noise}}}, \tag{9}$$

where γ represents SNR, n denotes the PL exponent, P_{noise} denotes the total additive noise power, and P_T represents the transmit power; $\beta = G_T G_R c^2/(4\pi f_o)^2$ denotes a constant value, where c represents the speed of light; G_R and G_T stand for the RX and TX gains, respectively. During the measurement, omnidirectional antennas were employed, therefore, we set $G_R = 1$ and $G_T = 1$. f_o presents the carrier frequency. In equation (9), the noise power P_{noise} is defined as $P_{\text{noise}} = K_b TB$, where T stands for temperature in K, B denotes the transmission bandwidth, and $K_b = 1.38 * 10^{(-23)}$ J/K denotes the Boltzmann constant.

It is assumed that $E\{W^2\} = 1$, the received average SNR $\bar{\gamma}$ with distance d can be written as [21]:

$$\bar{\gamma} = \frac{\beta P_T}{d^n P_{\text{noise}}}. \tag{10}$$

Given the condition that the received signal magnitude follows the Nakagami distribution. The PDF of the received signal magnitude w is defined as [71]:

$$f_w(w; m, \Omega) = \frac{2m^m w^{2m-1}}{\Omega^m \Gamma(m)} \exp\left(\frac{-mw^2}{\Omega}\right), \tag{11}$$

where $w \geq 0$ denotes the received signal magnitude and m is the shape factor, which determines the severity of channel fade. When m is equal to 1, the distribution yields to the Rayleigh distribution. When < 1, the distribution yields more severe fading. Ω is the scale parameter and $\Gamma(\cdot)$ represents the Gamma function.

Furthermore, the PDF of the received SNR considering the Nakagami fading model can be written as [25]:

$$f_\gamma(\gamma) = \left(\frac{m}{\bar{\gamma}}\right)^m \frac{\gamma^{m-1}}{\Gamma(m)} \exp\left(\frac{-m\gamma}{\bar{\gamma}}\right), \tag{12}$$

where m denotes the shape factor, γ represents the received SNR, and $\bar{\gamma}$ denotes the average SNR.

When the received SNR γ is more than the given SNR threshold Ψ, the vehicles are connected, and the transmitted message can be decoded correctly. Therefore, the probability of accurately received transmitted information at a distance d is as follows:

$$\begin{aligned} P(\gamma(d) \geq \Psi) &= \int_\Psi^\infty f_\gamma(\gamma) \mathrm{d}\gamma \\ &= \int_\Psi^\infty \left(\frac{m}{\bar{\gamma}}\right)^m \frac{\gamma^{m-1}}{\Gamma(m)} \exp\left(\frac{-m\gamma}{\bar{\gamma}}\right) \mathrm{d}\gamma \\ &= \frac{\Gamma(m, m\Psi/\gamma)}{\Gamma(m)}, \end{aligned} \tag{13}$$

where $\Gamma(m, m\Psi/\bar{\gamma})$ represents the incomplete Gamma function:

$$\Gamma(m, m\Psi/\bar{\gamma}) = \int_\Psi^\infty \left(\frac{m}{\bar{\gamma}}\right)^m \gamma^{m-1} \exp\left(\frac{-m\gamma}{\bar{\gamma}}\right) \mathrm{d}\gamma. \tag{14}$$

If m is a positive integer, $\Gamma(m) = (m-1)!$. $\Gamma(m, a)$ is calculated by [75]:

$$\Gamma(m, a) = (m-1)! \times e^{-a} \sum_{k=0}^{m-1} \frac{a^k}{k!}. \tag{15}$$

Together with equation (15), equation (13) can be further modified and represented as follows:

$$P(\gamma(d) \geq \Psi) = e^{\left(-m\Psi d^n P_{\text{noise}}/\beta P_T\right)} \sum_{k=0}^{m-1} \frac{\left(m\Psi d^n P_{\text{noise}}/\beta P_T\right)^k}{k!}, \tag{16}$$

where β is a constant value, P_T denotes the transmit power, m stands for the shape factor of the Nakagami distribution, n denotes the PL exponent, Ψ stands for the SNR threshold value, and P_{noise} represents the noise power.

In [22], authors considered the vehicle connectivity performance of two consecutive cars, however, the V2V connectivity between any two vehicles is not analyzed. Inspired by [22], we extend the two adjacent vehicles to any two vehicles to analyze the vehicle connectivity in the 1D VANET. In this paper, we consider that a wireless radio link is established if SNR γ is larger than the given SNR threshold value Ψ. The probability that the vehicle and its q-th neighboring vehicle are connected is given by

$$\begin{aligned} P_{si} &= P\left(\gamma(x) \geq \Psi \middle| Z_q = x\right) \\ &= \int_\Psi^\infty \int_0^\infty f_\gamma(\gamma) \cdot f_{Z_q}(x; q) \mathrm{d}x \, \mathrm{d}\gamma \\ &= \int_\Psi^\infty \int_0^\infty \left(\frac{m}{\bar{\gamma}}\right)^m \frac{\gamma^{m-1}}{\Gamma(m)} e^{-\left(\frac{m\gamma}{\bar{\gamma}} + \rho x\right)} x^{q-1} \mathrm{d}x \, \mathrm{d}\gamma \\ &\quad \cdot \frac{\rho^q}{(q-1)!}. \end{aligned} \tag{17}$$

After calculation, equation (17) becomes

$$P_{si} = \int_{\Psi}^{\infty}\int_{0}^{\infty} f_{\gamma}(\gamma) f_{Z_q}(x;q)\mathrm{d}x\,\mathrm{d}\gamma = \frac{\rho^q}{(q-1)!}\sum_{k=0}^{m-1}\left[\frac{\left(m\Psi P_{\text{noise}}/\beta P_T\right)^k}{k!}\cdot W_1\right], \tag{18}$$

where

$$W_1 = \int_0^{\infty} e^{-\left(\left(m\Psi P_{\text{noise}} x^n/\beta P_T\right)+\rho x\right)} x^{nk+q-1}\mathrm{d}x. \tag{19}$$

There is an integral term in equation (18), and the integral term is complicated to calculate. In this paper, we consider the derivation in [22] to calculate the integral in equation (18). The integral is given by

$$\int_0^{\infty} x^{t-1} e^{-\left(ux+sx^b\right)}\mathrm{d}x = (2\pi)^{(1-b/2)} b^{t-(1/2)} u^{-t} \times G_{1,b}^{b,1}\left(\frac{u^b}{s b^b}\middle|\begin{matrix}1\\ \\ \frac{t}{b},\ldots,\frac{t+b-1}{b}\end{matrix}\right), \tag{20}$$

where $G_{r,j}^{c,l}$ is the Meijers G function, t and u are greater than 0, s is also bigger than 0. It should be noted that equation (20) is valid when b is a positive integer value. Taking equation (20) into equation (18), we obtain

$$P_S = W_2\sum_{k=0}^{m-1}\frac{\left(m\Psi P_{\text{noise}}/\beta P_T\right)^k}{k!} n^{nk+q-1/2}\rho^{-(nk+q)} \times G_{1,n}^{n,1}\left(\frac{\rho^n\beta P_T}{m\Psi P_{\text{noise}} n^n}\middle|\begin{matrix}1\\ \\ \frac{nk+q}{n},\ldots,\frac{n(k+1)+q-1}{n}\end{matrix}\right), \tag{21}$$

with

$$W_2 = \frac{\rho^q}{(q-1)!}(2\pi)^{1-n/2}, \tag{22}$$

where β is a constant value, n denotes the PL exponent, and P_T stands for the transmit power. ρ denotes average vehicle density, m is the shape factor of the Nakagami distribution, Ψ denotes the SNR threshold value, and P_{noise} represents the noise power.

Therefore, for integer values of n and m, there exists the closed-form solution to the connectivity probability given by equation (21). However, for noninteger values of n and m, it is very hard to acquire a closed-loop solution to equation (17). Equation (21) is also the innovation point of this paper. The closed-loop expression of the V2V connectivity probability between any two vehicles under Nakagami-m fading is not given by others.

A special case would be with two consecutive vehicles, where the consecutive vehicle distance obeys an exponential distribution; its PDF is $f_{X_i}(x)$. As a result, the probability of two consecutive vehicles connected is calculated as [22]

$$\begin{aligned} P_c &= P\left(\gamma(x)\ge\Psi|X_i = x\right)\\ &= \int_{\Psi}^{\infty}\int_0^{\infty} f_{\gamma}(\gamma) f_{X_i}(x)\mathrm{d}x\,\mathrm{d}\gamma\\ &= \rho\int_0^{\infty} e^{-\rho x}\frac{\Gamma(m, m\Psi/\bar{\gamma})}{\Gamma(m)}\mathrm{d}x\\ &= \rho\sum_{k=0}^{m-1}\frac{\left(m\Psi P_{\text{noise}}/\beta P_T\right)^k}{k!}\int_0^{\infty} e^{-\left(\rho x+m\Psi x^n P_{\text{noise}}/\beta P_T\right)} x^{nk}\mathrm{d}x, \end{aligned} \tag{23}$$

where n denotes the PL exponent, P_T denotes the transmit power, P_{noise} is the noise power, ρ denotes average vehicle density, and Ψ denotes the SNR threshold value. β is a constant value and $\beta = G_T G_R c^2/(4\pi f_o)^2$.

For integer values of n, taking equation (20) into equation (23) results in [22]

$$P_c = \rho(2\pi)^{1-n/2}\sum_{k=0}^{m-1}\frac{\left(m\Psi P_{\text{noise}}/\beta P_T\right)^k}{k!} n^{nk+1/2}\rho^{-nk-1} \times G_{1,n}^{n,1}\left(\frac{\rho^n\beta P_T}{m\Psi P_{\text{noise}} n^n}\middle|\begin{matrix}1\\ \\ \frac{nk+1}{n},\ldots,\frac{n(k+1)}{n}\end{matrix}\right). \tag{24}$$

Therefore, in this special case the closed-form solution to the V2V connectivity probability of two consecutive vehicles in equation (23) is written as equation (24).

5.3. Impact of Nakagami-m Fading on V2V Connectivity. VANET connectivity is a function of vehicle mobility, vehicle density, SNR threshold, transmit power, and channel fading parameters. These parameters are directly correlated with the connectivity. In the following, we will discuss the influences of these parameters on V2V connectivity.

In this section, we set $\beta = 2.1 * 10^{-5}$, average vehicle density $\rho = 0.02$ vehicles/m, the transmit power $P_T = 37$ dBm, PL exponent $n = 1.785$, and the shape factor of the Nakagami distribution m ranges from 1 to 10. Figure 11 shows the effect of Nakagami fading parameter m on the proposed V2V connectivity probability. Simulation results showed that as m increases, the V2V connectivity probability increases. Therefore, the Nakagami fading parameter m has a positive effect on V2V connectivity performance.

Figure 12 shows the influence of the SNR threshold Ψ on connectivity probability. Results showed that the SNR threshold has a significant impact on V2V connectivity. A larger SNR threshold Ψ results in a smaller V2V connectivity probability. This finding is consistent with the earlier conclusion in [21].

Furthermore, the impact of average vehicle density on the V2V connectivity under Nakagami fading is illustrated in Figure 13, where ρ ranges from 0.001 to 0.1 vehicles/m. The result shows that the variations in vehicle density impact the communications' connectivity of the VANET. In free traffic state, the V2V connectivity probability increases with increasing vehicle density.

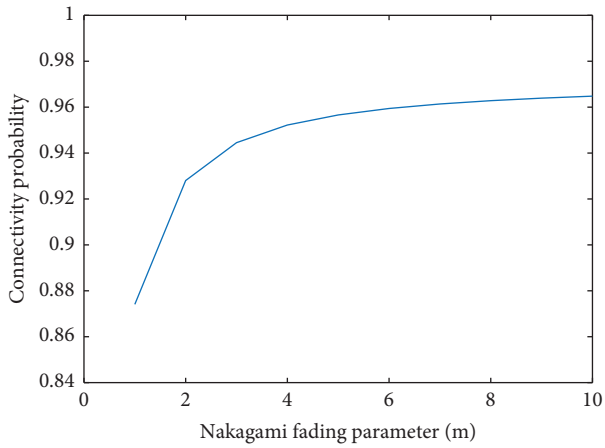

Figure 11: The connectivity probability versus fading parameter m.

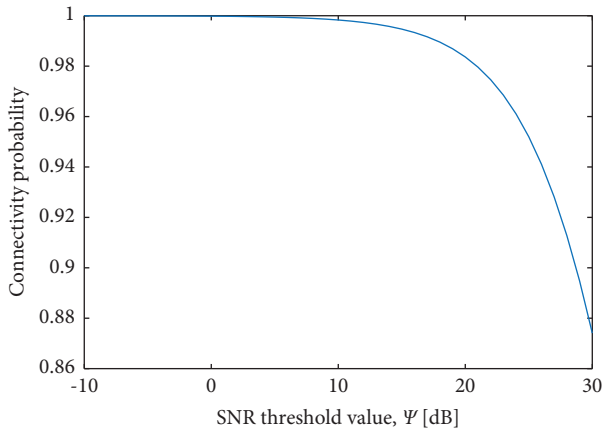

Figure 12: The connectivity probability versus SNR threshold Ψ.

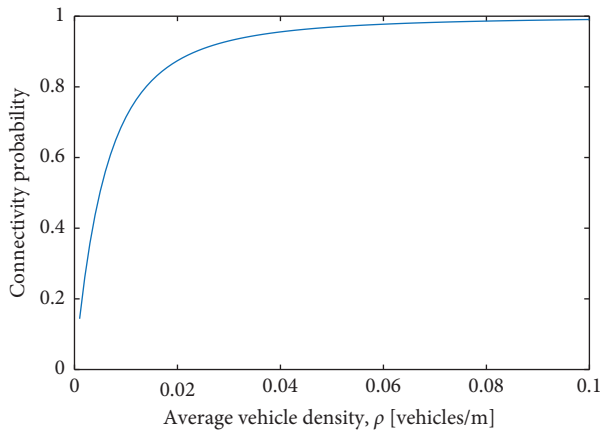

Figure 13: The connectivity probability with various ρ.

Figure 14 illustrates the results of relation between the connectivity probability and the transmit power P_T, where we can conclude that increasing the transmit power enhances the connectivity probability. Figure 15 shows the dependency between single-link connectivity probability and the neighbors' order q in the Nakagami fading channel.

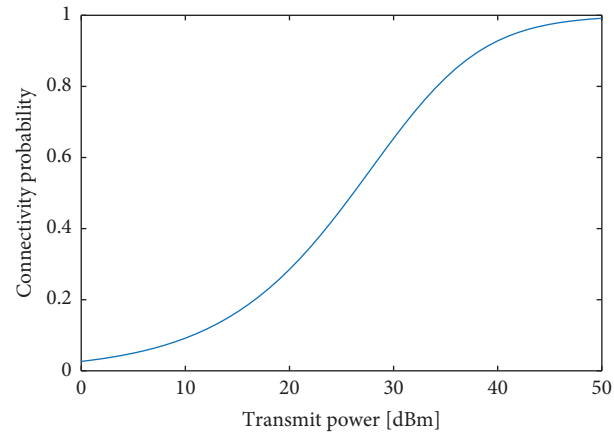

Figure 14: The influence of P_T on connectivity probability.

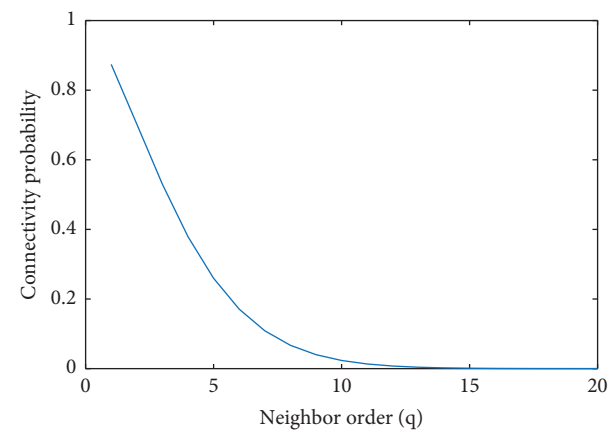

Figure 15: The connectivity probability versus neighbor order.

The result shows that the connectivity is significantly influenced by the neighbors' order. The farther neighbors' results in lower connectivity probability.

6. Conclusion

In this paper, we studied the V2V connectivity models considering the log-distance PL model and Nakagami-m fading model based on measurement results. First, we analyzed the channel characteristics in the tunnel, and found that compared to Rice, Rayleigh, Weibull, normal, and log-normal distributions, the Nakagami-m distribution is the best fit distribution for the signal amplitude fading in the tunnel scenario. Based on this finding, for the integer path loss exponent and fading factor, we derived a closed-form solution for the V2V connectivity probability of any two vehicles under the Nakagami channel. In addition, we studied the influences of large-scale and small-scale fading parameters on V2V connectivity performance. A bigger shape factor of Nakagami fading will result in a larger connectivity probability. The neighbor order also affect the vehicle connectivity in the VANET. The higher the neighbor order, the smaller the connectivity probability. If the PL exponent increases, the V2V connectivity probability

decreases. The shadow fading has a positive impact on connectivity probability. When the path loss threshold increases, the V2V connectivity probability increases, whereas if the SNR threshold increases, the connectivity probability decreases in Nakagami fading. Furthermore, we analyzed the influences of transmit power, transmission distance, and traffic parameters on V2V connectivity. Results showed that the higher the transmit power, the greater the connectivity probability. A larger transmission distance will bring smaller V2V connectivity probability. In free traffic flow, the V2V connectivity probability increases with increasing vehicle density.

Data Availability

The data used to support the findings of this study are included within the paper.

Conflicts of Interest

The authors declare that there are no conflicts of interest regarding the publication of this paper.

Acknowledgments

This research was funded by the Key Research and Development Program of Shaanxi under Grant 2021KWZ-08, the Scientific Research Program Funded by Shaanxi Provincial Education Department under Grant 22JK0248, the Innovation Capability Support Program of Shaanxi (Program No. 2022TD-41), the National Natural Science Foundation of China under Grant 61871059, and the Fundamental Research Funds for the Central Universities under Grant 300102249302.

References

[1] F. Li, W. Chen, and Y. Shui, "Connectivity probability analysis of VANETs at different traffic densities using measured data at 5.9 GHz," *Physical Communication*, vol. 35, no. 10, pp. 1–11, 2019.

[2] Q. Wu, S. Shi, Z. Wan, Q. Fan, P. Fan, and C. Zhang, "Towards V2I age-aware fairness access: a dqn based intelligent vehicular node training and test method," *Chinese Journal of Electronics*, vol. 2022, no. 1, pp. 1–30, 2022.

[3] Q. Wu, Y. Zhao, Q. Fan, P. Fan, J. Wang, and C. Zhang, "Mobility-Aware cooperative caching in vehicular edge computing based on asynchronous federated and deep reinforcement learning," *IEEE Journal of Selected Topics in Signal Processing*, vol. 16, 2022.

[4] P. K. Sahoo, M. Chiang, and S. Wu, "Connectivity modeling of vehicular ad hoc networks in signalized city roads," in *Proceedings of the 2011 40th International Conference on Parallel Processing Workshops*, pp. 22–26, Taipei, Taiwan, September 2011.

[5] C. Bian, J. Zhao, X. Sun, X. Li, and D. Zou, "Network connectivity performance analysis of platoon-based vehicular adhoc network on a two-way lane," in *Proceedings of the 2019 IEEE International Conference on Signal, Information and Data Processing (ICSIDP)*, pp. 1–5, Chongqing, China, December 2019.

[6] H. Füßler, M. Torrent-Moreno, M. Transier, R. Kruger, H. Hartenstein, and W. Effelsberg, "Studying vehicle movements on highways and their impact on ad-hoc connectivity," *ACM SIGMOBILE - Mobile Computing and Communications Review*, vol. 10, no. 4, pp. 26-27, 2006.

[7] M. Khabazian and M. K. M. Ali, "A performance modeling of connectivity in vehicular ad hoc networks," *IEEE Transactions on Vehicular Technology*, vol. 57, no. 4, pp. 2440–2450, 2008.

[8] Z. Khan, P. Fan, and S. Fang, "On the connectivity of vehicular ad hoc network under various mobility scenarios," *IEEE Access*, vol. 5, pp. 22559–22565, 2017.

[9] S. Durrani, X. Zhou, and A. Chandra, "Effect of vehicle mobility on connectivity of vehicular ad hoc networks," in *Proceedings of the Vehicular Technology Conference Fall*, pp. 1–5, Ottawa, ON, Canada, September 2010.

[10] I. Ho, K. K. Leung, J. W. Polak, and R. Mangharam, "Node connectivity in vehicular ad hoc networks with structured mobility," in *Proceedings of the IEEE Conference on Local Computer Networks*, pp. 1–8, Dublin, Ireland, October 2007.

[11] X. Hou, Y. Li, D. Jin, D. O. Wu, and S. Chen, "Modeling the impact of mobility on the connectivity of vehicular networks in large-scale urban environments," *IEEE Transactions on Vehicular Technology*, vol. 65, no. 4, pp. 2753–2758, 2016.

[12] C. Chen, L. Liu, X. Du, X. Wei, and C. Pei, "Available connectivity analysis under free flow state in VANETs," *EURASIP Journal on Wireless Communications and Networking*, vol. 2012, pp. 270–319, 2012.

[13] B. Pan and H. Wu, "Analysis of conditional connectivity based on two lanes for VANETs," in *Proceedings of the International Conference on Communications and Networking in China*, pp. 532–541, Springer, Xi'an, China, October 2017.

[14] S. C. Ng, W. Zhang, Y. Yang, and G. Mao, "Analysis of access and connectivity probabilities in infrastructure-based vehicular relay networks," in *Proceedings of the 2010 IEEE Wireless Communication and Networking Conference*, pp. 1–6, Sydney, NSW, Australia, April 2010.

[15] S. C. Ng, W. Zhang, Y. Zhang, Y. Yang, and G. Mao, "Analysis of access and connectivity probabilities in vehicular relay networks," *IEEE Journal on Selected Areas in Communications*, vol. 29, no. 1, pp. 140–150, 2011.

[16] C. Shao, S. Leng, Y. Zhang, A. Vinel, and M. Jonsson, "Performance analysis of connectivity probability and connectivity-aware MAC protocol design for platoon-based VANETs," *IEEE Transactions on Vehicular Technology*, vol. 64, no. 12, pp. 5596–5609, 2015.

[17] R. Chen, Z. Sheng, Z. Zhong, M. Ni, D. G. Michelson, and V. C. M. Leung, "Analysis on connectivity performance for vehicular ad hoc networks subjected to user behavior," in *Proceedings of the 2015 International Wireless Communications and Mobile Computing Conference (IWCMC)*, pp. 26–31, Dubrovnik, Croatia, August, 2015.

[18] B. Pan and H. Wu, "Performance analysis of connectivity considering user behavior in V2V and V2I communication systems," in *Proceedings of the 2017 IEEE 86th Vehicular Technology Conference (VTC-Fall)*, pp. 1–5, Toronto, ON, Canada, September 2017.

[19] D. Miorandi and E. Altman, "Coverage and connectivity of ad hoc networks presence of channel randomness," in *Proceedings of the IEEE 24th Annual Joint Conference of the IEEE Computer and Communications Societies*, pp. 491–502, Miami, FL, USA, March 2005.

[20] N. P. Chandrasekharamenon and B. Ancharev, "Connectivity analysis of one-dimensional vehicular ad hoc networks in

fading channels," *EURASIP Journal on Wireless Communications and Networking*, vol. 2012, no. 1, pp. 1–16, 2012.

[21] A. V. Babu and V. K. Muhammed Ajeer, "Analytical model for connectivity of vehicular ad hoc networks in the presence of channel randomness," *International Journal of Communication Systems*, vol. 26, no. 7, pp. 927–946, 2013.

[22] N. M. Mathew and P. C. Neelakantan, "Analyzing the Network connectivity probability of a linear VANET in Nakagami fading channels," in *Proceedings of the International Conference on Distributed Computing and Networking*, pp. 505–511, Kharagpur India, January 2014.

[23] S. Elaraby and S. M. Abuelenin, "Fading improves connectivity in vehicular ad-hoc networks," 2019, https://arxiv.org/abs/1910.05317.

[24] L. Zhang, Y. Zhang, M. Ma, and Y. Guan, "An analysis of K-connectivity in shadowing and Nakagami fading wireless multi-Hop networks," in *Proceedings of the VTC Spring 2008 - IEEE Vehicular Technology Conference*, pp. 395–399, Marina Bay, Singapore, May, 2008.

[25] S. M. Hanshi, M. M. Kadhum, and T. C. Wan, "On connectivity analysis of vehicular ad hoc networks in presence of channel randomness," in *Proceedings of the 4th International Conference on Internet Applications, Protocols and Services (NETAPPS2015)*, pp. 94–99, CyberJaya, Malaysia, December, 2015.

[26] S. Jiang, W. Wang, and I. Rashdan, "V2V channel modeling at 5.2 GHz for highway environment," *China Communications*, vol. 19, no. 11, pp. 112–128, 2022.

[27] R. Chen and Z. Zhong, "Analysis on V2V connectivity under dual-slope path loss model in urban scenarios," in *Proceedings of the 2014 URSI General Assembly and Scientific Symposium (URSI GASS)*, pp. 1–4, Beijing, China, August, 2014.

[28] R. Chen, Z. Zhong, V. C. M. Leung, and D. G. Michelson, "Performance analysis of connectivity for vehicular ad hoc networks with moving obstructions," in *Proceedings of the 2014 IEEE 80th Vehicular Technology Conference (VTC2014-Fall)*, pp. 1–5, Vancouver, BC, Canada, September, 2014.

[29] D. Miorandi, E. Altman, and G. Alfano, "The impact of channel randomness on coverage and connectivity of ad hoc and sensor networks," *IEEE Transactions on Wireless Communications*, vol. 7, no. 3, pp. 1062–1072, 2008.

[30] R. S. Tomar and M. S. Sharma, "Connectivity analysis in vehicular communication for safe transportation systems," in *Proceedings of the 2017 Conference on Information and Communication Technology (CICT)*, pp. 1–5, Gwalior, India, November, 2017.

[31] S. Yousefi, E. Altman, R. El-Azouzi, and M. Fathy, "Analytical model for connectivity in vehicular ad hoc networks," *IEEE Transactions on Vehicular Technology*, vol. 57, no. 6, pp. 3341–3356, 2008.

[32] G. H. Mohimani, F. Ashtiani, A. Javanmard, and M. Hamdi, "Mobility modeling, spatial traffic distribution, and probability of connectivity for sparse and dense vehicular ad hoc networks," *IEEE Transactions on Vehicular Technology*, vol. 58, no. 4, 2009.

[33] D. Miorandi and E. Altman, "Connectivity in one-dimensional ad hoc networks: a queueing theoretical approach," *Wireless Networks*, vol. 12, no. 5, pp. 573–587, 2006.

[34] S. Yousefi, E. Altman, R. El-Azouzi, and M. Fathy, "Improving connectivity in vehicular ad hoc networks: an analytical study," *Computer Communications*, vol. 31, no. 9, pp. 1653–1659, 2008.

[35] H. Yousefi'zadeh, H. Jafarkhani, and J. Kazemitabar, "A study of connectivity in MIMO fading ad-hoc networks," *Journal of Communications and Networks*, vol. 11, no. 1, pp. 47–56, 2009.

[36] W. Zhang, Y. Chen, Y. Yang et al., "Multi-hop connectivity probability in infrastructure-based vehicular networks," *IEEE Journal on Selected Areas in Communications*, vol. 30, no. 4, pp. 740–747, 2012.

[37] F. Li, W. Chen, J. Wang et al., "Different traffic density connectivity probability analysis in VANETs with measured data at 5.9 GHz," in *Proceedings of the 2018 16th International Conference on Intelligent Transportation Systems Telecommunications (ITST)*, pp. 1–7, Lisboa, Portugal, October, 2018.

[38] Y. Wang and J. Zheng, "A connectivity analytical model for a highway with an entrance/exit in vehicular ad hoc networks," in *Proceedings of the 2016 IEEE International Conference on Communications (ICC)*, pp. 1–6, Kuala Lumpur, Malaysia, May, 2016.

[39] Y. Wang and J. Zheng, "Connectivity analysis of a highway with one entry/exit and multiple roadside units," *IEEE Transactions on Vehicular Technology*, vol. 67, no. 12, pp. 11705–11718, 2018.

[40] S. Kwon, Y. Kim, and N. B. Shroff, "Analysis of connectivity and capacity in 1-D vehicle-to-vehicle networks," *IEEE Transactions on Wireless Communications*, vol. 15, no. 12, pp. 8182–8194, 2016.

[41] J. Zhao, Y. Chen, and Y. Gong, "Study of connectivity probability based on cluster in vehicular ad hoc networks," in *Proceedings of the 2016 8th International Conference on Wireless Communications Signal Processing (WCSP)*, pp. 1–5, Yangzhou, China, October, 2016.

[42] H. Xiao, Q. Zhang, S. Ouyang, and A. T. Chronopoulos, "Connectivity probability analysis for VANET way traffic using a cell transmission model," *IEEE Systems Journal*, vol. 15, no. 2, pp. 1815–1824, 2021.

[43] V. A. Aalo and C. Mukasa, "Impact of interference on the coverage and connectivity of ad hoc networks in a fading environment," *AEU-International Journal of Electronics and Communications*, vol. 69, no. 8, pp. 1094–1101, 2015.

[44] D. B. Rawat and B. Chandra, "Adaptive connectivity for spectrum agile VANETs in fading channels," in *Vehicular Cyber Physical Systems*Springer, Berlin, Germany, 2017.

[45] M. Pradeep, P. S. David, and P. Jacob, "One dimensional vehicular ad-hoc network connectivity analysis under fading conditions," *Procedia Computer Science*, vol. 115, pp. 615–625, 2017.

[46] G. Yan and B. Danda, "Rawat. "Vehicle-to-vehicle connectivity analysis for vehicular ad-hoc networks"," *Ad Hoc Networks*, vol. 58, pp. 25–35, 2016.

[47] S. Hussain, D. Wu, W. Xin, S. Memon, N. Khuda, and A. Saleem, "Reliability and connectivity analysis of vehicluar ad hoc networks for a highway tunnel," *International Journal of Advanced Computer Science and Applications*, vol. 10, no. 4, pp. 181–186, 2019.

[48] P. Golmohammadi, P. Mokhtarian, F. Safaei, and R. Raad, "An analytical model of network connectivity in vehicular ad hoc networks using spatial point processes," in *Proceedings of the IEEE International Symposium on a World of Wireless, Mobile and Multimedia Networks*, pp. 1–6, Sydney, NSW, Australia, June, 2014.

[49] J. Zhao, Y. Chen, and Y. Gong, "Study of connectivity probability of vehicle-to-vehicle and vehicle-to-infrastructure communication systems," in *Proceedings of the 2016 IEEE 83rd Vehicular Technology Conference (VTC Spring)*, pp. 1–4, Nanjing, China, May, 2016.

[50] B. Xu and Z. Qi, "Analysis of connectivity in ad hoc network with nakagami-m fading," in *Proceedings of the 2014 International Conference on Information Science Electronics and Electrical Engineering*, vol. 3, pp. 1609–1612, Sapporo, Japan, April, 2014.

[51] S. M. Abuelenin and S. Elaraby, "A generalized framework for connectivity analysis in vehicle-to-vehicle communications," *IEEE Transactions on Intelligent Transportation Systems*, vol. 23, no. 6, pp. 5894–5898, 2022.

[52] F. Li, W. Chen, and Y. Shui, "Study on connectivity probability of VANETs under adverse weather conditions at 5.9 GHz," *IEEE Access*, vol. 8, pp. 547–555, 2020.

[53] A. Jia, S. Jiang, L. v. Yue et al., "Connectivity analysis of V2V channel at intersections," in *Proceedings of the 2021 15th European Conference on Antennas and Propagation (EuCAP)*, pp. 1–4, Dusseldorf, Germany, March, 2021.

[54] S. C. Ng, G. Mao, and B. D. O. Anderson, "On the properties of one-dimensionalinfrastructure-based wireless multi-hop networks," *IEEE Transactions on Wireless Communications*, vol. 11, no. 7, pp. 2606–2615, 2012.

[55] J. Cheng, G. Yuan, M. Zhou, S. Gao, Z. Huang, and C. Liu, "A connectivity-prediction-based dynamic clustering model for VANET in an urban scene," *IEEE Internet of Things Journal*, vol. 7, no. 9, pp. 8410–8418, 2020.

[56] C. Li, A. Zhen, J. Sun, M. Zhang, and X. Hu, "Analysis of connectivity probability in VANETs considering minimum safety distance," in *Proceedings of the 2016 8th International Conference on Wireless Communications Signal Processing (WCSP)*, pp. 1–5, Yangzhou, China, October 2016.

[57] L. Cheng and S. Panichpapiboon, "Effects of intervehicle spacing distributions on connectivity of VANET: a case study from measured highway traffic," *IEEE Communications Magazine*, vol. 50, no. 10, pp. 90–97, 2012.

[58] W. Viriyasitavat, O. K. Tonguz, and F. Bai, "Network connectivity of VANETs in urban areas," in *Proceedings of the 2009 6th Annual IEEE Communications Society Conference on Sensor, Mesh and Ad Hoc Communications and Networks*, pp. 1–9, Rome, Italy, June, 2009.

[59] M. G. Almiron, O. Goussevskaia, A. C. Frery, and A. A. F. Loureiro, "Connectivity at crossroads," in *Proceedings of the 2014 IEEE 25th Annual International Symposium on Personal, Indoor, and Mobile Radio Communication (PIMRC)*, pp. 1437–1441, Washington, DC, USA, September, 2014.

[60] Y. Regragui and N. Moussa, "Impact of mobility design on network connectivity dynamics in urban environment," *Simulation Modelling Practice and Theory*, vol. 119, Article ID 102577, 26 pages, 2022.

[61] J. Naskath, B. Paramasivan, and H. Aldabbas, "A study on modeling vehicles mobility with MLC for enhancing vehicle-to-vehicle connectivity in VANET," *Journal of Ambient Intelligence and Humanized Computing*, vol. 12, no. 8, pp. 8255–8264, 2021.

[62] M. Gramaglia, O. Trullols-Cruces, D. Naboulsi, M. Fiore, and M. Calderon, "Mobility and connectivity in highway vehicular networks: a case study in Madrid," *Computer Communications*, vol. 78, pp. 28–44, 2016.

[63] P. B. Bautista, L. Urquiza-Aguiar, and M. . Aguilar Igartua, "Evaluation of dynamic route planning impact on vehicular communications with SUMO," in *Proceedings of the 23rd International ACM Conference on Modeling, Analysis and Simulation of Wireless and Mobile Systems*, pp. 27–35, Alicante, Spain, November, 2020.

[64] X. Jin, W. Su, and W. Yan, "Quantitative analysis of the VANET connectivity: theory and application," in *Proceedings of the 2011 IEEE 73rd Vehicular Technology Conference (VTC Spring)*, pp. 1–5, IEEE, Budapest, Hungary, May, 2011.

[65] S. Jat, R. S. Tomar, and M. S. P. Sharma, "Traffic congestion and accident prevention analysis for connectivity in vehicular ad-hoc network," in *Proceedings of the 2019 5th International Conference on Signal Processing, Computing and Control (ISPCC)*, pp. 185–190, Solan, India, October, 2019.

[66] S. I. Sou and O. K. Tonguz, "Enhancing VANET connectivity through roadside units on highways," *IEEE Transactions on Vehicular Technology*, vol. 60, no. 8, pp. 3586–3602, 2011.

[67] T. Abbas, K. Sjoberg, J. Karedal, and F. Tufvesson, "A measurement based shadow fading model for vehicle-to-vehicle network simulations," *International Journal of Antennas and Propagation*, vol. 2015, Article ID 190607, 12 pages, 2015.

[68] C. Li, K. Yang, J. Yu et al., "V2V radio channel performance based on measurements in ramp scenarios at 5.9 GHz," *IEEE Access*, vol. 6, pp. 7503–7514, 2018.

[69] Ke Guan, Bo Ai, Z. Zhong et al., "Measurements and analysis of large-scale fading characteristics in curved subway tunnels at 920 MHz, 2400 MHz, and 5705 MHz," *IEEE Transactions on Intelligent Transportation Systems*, vol. 16, no. 5, pp. 2393–2405, 2015.

[70] I. Hussain, F. Cawood, and R. van Olst, "Effect of tunnel geometry and antenna parameters on through-the-air communication systems in underground mines: survey and open research areas," *Physical Communication*, vol. 23, pp. 84–94, 2017.

[71] R. He, A. F. Molisch, F. Tufvesson, Z. Zhong, B. Ai, and T. Zhang, "Vehicle-to-vehicle propagation models with large vehicle obstructions," *IEEE Transactions on Intelligent Transportation Systems*, vol. 15, no. 5, pp. 2237–2248, 2014.

[72] Ke Guan, Z. Zhong, J. I. Alonso, and C. Briso-Rodriguez, "Measurement of distributed antenna systems at 2.4 GHz in a realistic subway tunnel environment," *IEEE Transactions on Vehicular Technology*, vol. 61, no. 2, pp. 834–837, 2012.

[73] Y. Jia, M. Zhao, W. Zhou, and P. Dong, "Measurement and statistical analysis of 1.89 GHz radio propagation in a realistic mountain tunnel," in *Proceedings of the 2015 International Conference on Wireless Communications Signal Processing (WCSP)*, pp. 1–5, Nanjing China, October 2015.

[74] S. Jiang, T. Chang, A. Jia, and W. Wang, "A study on vehicle connectivity and its impact on positioning," in *Proceedings of the 2021 15th European Conference on Antennas and Propagation (EuCAP)*, pp. 1–5, Dusseldorf, Germany, March, 2021.

[75] I. S. Gradshteyn and I. M. Ryzhik, "Table of integrals, series, and products," *Table of Integrals*, 1, pp. 1161–1171, 103 edition, 2007.